Eulerian simulations of an iron dust Bunsen burner

Rizwan Mehmood*, Quentin Fradet, Uwe Riedel

German Aerospace Center (DLR), Institute of Low-Carbon Industrial Processes. Zittau, Germany

1) Novelty Statement

In this work, we model the combustion of iron particles through the usage of Eulerian fields. We use a sectional method to discretize the particle size distribution into bins, each bin representing particles of different diameters. Iron particle physics and oxidation chemistry strongly depend on particle diameter; this method allows us to model both accurately and efficiently without resolving a detailed particle size distribution. While the sectional approach itself is well-established, to the best of our knowledge we are the first to apply it to computational fluid dynamics (CFD) simulations of iron powder combustion.

2) Significance Statement

Even when using HPCs, traditional Lagrangian-based simulations of iron powder combustion bottleneck when simulating the immense numbers of particles present in industrial full-scale applications. Our work presents an alternative method that can scale to industrial-level CFD simulations without encountering these issues.

3) Author Contribution

- RM: performed research, analysed data, wrote paper
- QF: designed research, reviewed paper, supervision
- UR: designed research, reviewed paper, supervision

4) Preferred Presentation Format

The authors prefer an **oral presentation** for the following reasons: a) the work features visualizations of iron flames, which are easier to follow as videos than as still images; b) the work presents numerical simulations of prior experimental work and an oral presentation would aid us in placing the work in its proper scientific context; c) the mixture of fundamental iron combustion science and application-based analysis appeals to a broad audience and would benefit from wider exchanges over one-to-one discussions.

5) Colloquia Designation

Colloquium choices (in order of preference): a) Energy and Material Conversion and Heating Processes; b) Modelling Approaches; c) Heterogenous Combustion and Processes

Keywords: Iron dust burner, Metal combustion, Sectional approach, Eulerian approach

Eulerian simulations of an iron dust Bunsen burner

Rizwan Mehmood*, Quentin Fradet, Uwe Riedel

German Aerospace Center (DLR), Institute of Low-Carbon Industrial Processes, Zittau, Germany

Abstract

Computational Fluid Dynamics (CFD) simulations of iron powder combustion have thus far treated particles as Lagrangian objects, with implications for simulation scalability. Here, a fully-Eulerian model of iron powder combustion is presented, utilizing a sectional approach to express polydispersity. Featuring custom thermodynamics and representing phase changes as chemical reactions, the model is used to simulate an experimental iron dust Bunsen burner (Fedoryk *et al.*, 2023) and further compared to Lagrangian simulations thereof (Hazenberg *et al.*, 2026). Both single-phase and multiphase approaches are presented; single-phase simulations recover chemistry well, albeit with low laminar flame speeds comparable to those of iron powder combustion in microgravity. However, treatment of iron as being part of an ideal gas leads to inaccurate particle physics. Multiphase simulations recover particle physics well, displaying accurate uplift through buoyancy forces. However, the reaction rate of iron oxidation is much lower than that suggested by prior results. Outlet velocity distributions exhibit plug-like flow, with multiphase simulations doing so more strongly than single-phase simulations. Overall, reasonable agreement with prior results was obtained for single-phase simulations. Future work will involve increasing multiphase simulation accuracy, then scaling both up towards turbulent iron flames.

Keywords: CFD; Metal fuels; Sectional approach;

*Corresponding author.

1. Introduction

As German coal-fired power plants start nearing phase-out, the idea of retrofitting them is gaining traction. This would allow continued usage of existing infrastructure while also having sociopolitical benefits. For retrofitting to be environmentally beneficial, however, the new fuel would need to be CO_2-neutral. Alongside various biomass-based fuels that come into question, iron is a viable option. Iron powder could be combusted in retrofitted coal-fired power plants to release energy for steam generation. The iron oxide formed this way could be reduced by blue or even green hydrogen back to iron, giving rise to an "iron power cycle" and making iron a renewable carrier of renewable energy.

Efficiency comparisons between coal-fired power plants and retrofitted iron power plants show that retrofitting makes sense thermodynamically [1, 2]. Implementing this idea, however, requires knowledge of the optimal conditions and operating parameters, which in turn requires computational fluid dynamics (CFD) simulations of iron combustion in retrofitted power plants to be carried out. This is easier said than done: Current CFD simulations of iron combustion treat particles as Lagrangian objects, and resolving the large numbers of particles present in an industrial combustion chamber is beyond the capacity of current and future HPCs. Field representations of burning iron particles are possible in theory, but would not be able to resolve the polydispersity present in real iron powders. What is needed is a method to combine the high flexibility of Lagrangian simulations with the low computational cost of Eulerian representations.

This work presents CFD simulations of iron powder combustion, with polydispersity modelled through a sectional approach. This model is used to simulate an iron Bunsen burner, and validated against experimental and Lagrangian-CFD results.

2. Computational Methods

2.1 Sectional Approach

The sectional approach is a computational method for dealing with polydispersity in CFD. A continuous distribution is discretized through construction of bins, with transport equations being solved separately for each bin. A particle size distribution of spherical iron powder based on prior work [3] was used. The particle diameter was discretized due to its relevance to both the chemistry of iron combustion and the physics of iron powder in air. Six bins were constructed; with geometric constraints dictating a scaling factor of 2 between neighbouring bins [4, 5], the smallest bin was 0.75 µm and the largest 24 µm.

2.2 *Single-Phase Simulations*

Single-phase simulations were carried out in OpenFOAM v11 [6]. Only a single gas phase was modeled, with particles assumed to follow it perfectly (dusty gas model). The governing equations for this gaseous phase are the standard compressible Navier-Stokes equations, whereas the implemented kinetic mechanism reads:

$$\mathrm{Fe}^i_{(\mathrm{s})} \rightleftharpoons \mathrm{Fe}^i_{(\mathrm{l})} \quad (1)$$

$$0.5\ \mathrm{O}_2 + \mathrm{Fe}^i_{(\mathrm{l})} \rightarrow \mathrm{FeO}^i_{(\mathrm{l})} \quad (2)$$

$$\mathrm{FeO}^i_{(\mathrm{l})} \rightleftharpoons \mathrm{FeO}^i_{(\mathrm{s})} \quad (3)$$

The subscripts (l) and (s) refer to the liquid and solid phases, respectively. Custom thermodynamics [7] were used for ferrous species. Phase changes were treated as chemical reactions [8], with rate laws (e.g. solid iron formation) reading as follows:

$$\frac{\mathrm{d}\left[\mathrm{Fe}^i_{(\mathrm{s})}\right]}{\mathrm{d}t} = k_{-1}\left[\mathrm{Fe}^i_{(\mathrm{l})}\right] - k_1\left[\mathrm{Fe}^i_{(\mathrm{s})}\right] \quad (4)$$

k_n is the rate constant for the n^{th} forward reaction, k_{-n} is the rate constant for the n^{th} backward reaction (both in s^{-1}), and $\left[m^i\right]$ is the molar concentration of the i^{th} bin of the m^{th} species in $\mathrm{mol} \cdot \mathrm{L}^{-1}$. The rate law for the iron oxidation reaction reads:

$$r_{\mathrm{ox}} = k_\infty \exp\left(\frac{-T_{\mathrm{a}}}{T}\right) A^i_{\mathrm{p}} N_{\mathrm{p}} \left[\mathrm{O}_{2\,(\mathrm{g})}\right] \quad (5)$$

with k_∞ the pre-exponential factor, T the temperature in Kelvin, T_{a} the activation temperature in Kelvin, A^i_{p} the particle surface area of the i^{th} bin in m^2, and N_{p} the particle number density in m^{-3}. The oxidation rate law structure and parameters were taken from theoretical considerations [9] and validation studies [10, 11].

2.3 *Multiphase Simulations*

Multiphase simulations were carried out using MFiX [12], a CFD software specialized in simulations of granular materials. The gaseous and solid phases were modelled as separate Eulerian phases (Euler-Euler model) with separate sets of Navier-Stokes equations coupled through exchange terms such as drag force, buoyancy, and heterogenous chemistry. The granular energy balance of the solid phase, with both kinetic and frictional contributions, was also solved for.

Simplified chemical kinetics were implemented in MFiX. Only iron and iron oxide were considered, with no reference to phase changes; the mechanism and rate laws read:

$$0.5\ \mathrm{O}_2 + \mathrm{Fe}^i \rightarrow \mathrm{FeO}^i \quad (6)$$

$$r_{\mathrm{ox}} = k_\infty \exp\left(\frac{-T_{\mathrm{a}}}{T_{\mathrm{rct}}}\right) A^i_{\mathrm{p}} N_{\mathrm{p}} \left[\mathrm{O}_{2\,(\mathrm{g})}\right] \quad (7)$$

$$T_{\mathrm{rct}} = 0.5\left(T_{\mathrm{s}} + T_{\mathrm{g}}\right) \quad (8)$$

The temperature T_{rct} was taken as the mean of the solid phase temperature T_{s} and the gas phase temperature T_{g}, both in Kelvin. Species thermodynamics and rate law parameters were identical to those used in OpenFOAM.

3. Results and Discussion

3.1 *Single-Phase Simulations*

Figure 1 shows an iron flame as simulated in OpenFOAM. The left-hand side of the figure shows the molar excess of iron vs iron oxide: Black areas indicate an excess of iron, red an excess of iron oxide. White areas indicate equal amounts of both species. The right-hand side of the figure shows the heat release rate $\dot{Q}$ of the flame (in $\mathrm{J} \cdot \mathrm{s}^{-1}$). Bright yellow indicates areas of high heat release, darker colours are those of lower heat release. $\dot{Q}$ was clipped at the lower end at $10^4\ \mathrm{J} \cdot \mathrm{s}^{-1}$. Further, the temperature field around the flame is shown by the usage of contour lines: The innermost contour line represents 1800 K, whereas the outermost contour line represents 600 K. Iron is almost fully oxidized in the flame, as would be expected. The overall shape and structure of the flame agrees well with numerical [3] and experimental [13] results, with some caveats. In particular, the flame is continuous and not a collection of discrete burning particles. This can be attributed to the single-phase nature of the simulation.

Figure 2 shows the dependency of the laminar flame speed on the chosen temperature contour. The circles represent individual values, while the dotted line represents the mean value and the shaded area the standard deviation. The 900 K contour, which is

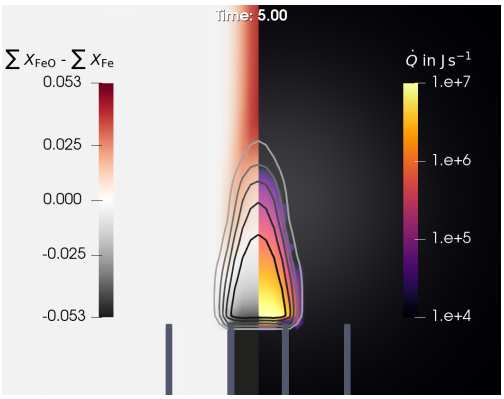


Figure 1: Molar excess (left), heat release rate (right) and temperature contours (lines) of an iron flame (OpenFOAM simulation).

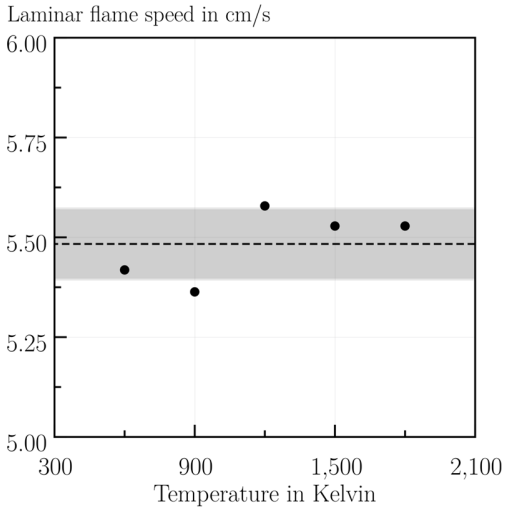


Figure 2: The laminar flame speed measured using different temperature contours: individual values (circles), mean (dotted line) and standard deviation (shaded area).

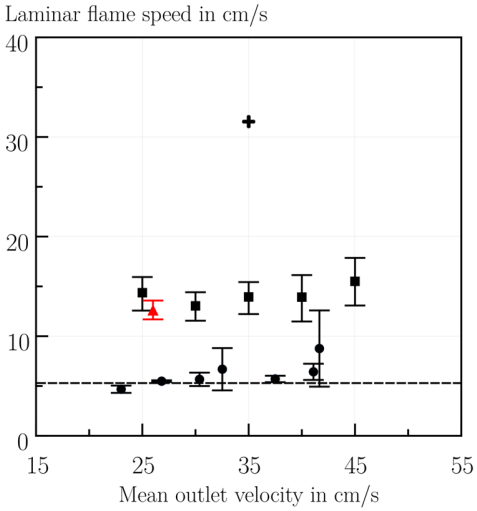


Figure 3: The laminar flame speed of iron dust flames: our work (circles), our single-bin value (cross), experimental results of the iron Bunsen burner [13] (squares), Lagrangian CFD results [3] (red triangle) and stationary iron flames in microgravity [14] (dashed line).

second from the outside in Figure 1, corresponds well with the area of $\dot{Q} > 10^4$ J · s^{-1}, which is represented by the entire coloured area within Figure 1. However, Figure 2 shows that the flame speed at 900 K is farthest from the mean flame speed. Hazenberg *et al.* [3] used a lower temperature contour to determine flame speed. They further showed that the variation of laminar flame speed with the chosen contour was minimal, which was also the case here.

The laminar flame speed as a function of mean outlet velocity, as reported by various authors, is shown in Figure 3. Our results using OpenFOAM are represented by black circles, with the uncertainty calculated through the usage of different temperature contours. The irregular x-value spacing of these results arises from OpenFOAM calculating the mean outlet velocity from a given inlet velocity boundary condition. The black cross is the value obtained by simulating a single bin in OpenFOAM. The black squares are experimental results for the iron Bunsen burner [13], with the uncertainty representing the experimental uncertainty reported by the authors. The red triangle is the value as determined by Lagrangian-CFD of the iron Bunsen burner [3], and has been shifted right for readability. The uncertainty assigned to this value is given by the usage of different methods to calculate the laminar flame speed. Finally, the dashed line represents the theoretical laminar flame speed of stationary iron dust flames in microgravity [14]. Our values are approximately half of the values obtained in both experiments and through Lagrangian simulations. Interestingly, our values lie close to the theoretical value predicted for microgravity environments. The experimental laminar flame speed obtained through combustion of iron powder in microgravity matches this theoretical value, and with it our obtained value, quite well [14]. This is due to our simulations treating iron as part of an ideal gas phase, and as a result being much less affected by gravity than in experiments and Lagrangian simulations. While the Navier-Stokes equations do include a gravitational term, the density of iron is calculated through the ideal gas equation, and as a result is hugely underestimated. This leads to much less gravitational force acting on the particles in our simulation than would do so physically. In short, while the chemistry is accurate, the physics are not.

3.2 Multiphase Simulations

The results of multiphase simulations in MFiX are shown in Figure 4. The left-hand side shows solids volume fraction as a proportion of maximum solids volume fraction, while the right-hand side shows the reaction rate of the oxidization of iron to iron oxide. The physics of particles in air are well-reproduced, with iron spilling out over the side of the burner as it reaches the outlet. The co-flow produces further lift on the particles, causing the “bounce” seen in the image. However, not all particles are uplifted, which is why a low volume fraction of particles is in the co-flow tube. Despite all reactants entering the domain at elevated temperatures, the reaction rate is low overall, with no significant amounts of iron oxide produced. Further, a flame cannot be observed, and no ignition event takes place. The acceleration of the flow through a flame would provide a further source of lift to the particles, and explains the discrepancy between this work, where the particles spill over the side of the

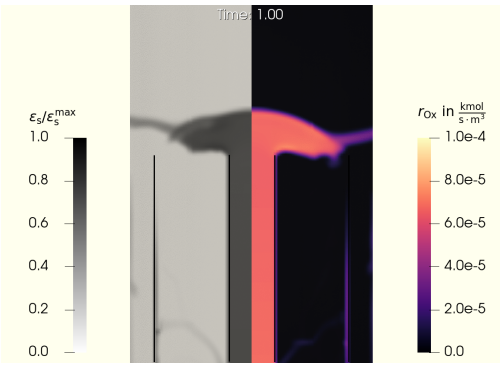


Figure 4: Solids volume fraction (left) and reaction rate (right) of an iron flame (MFiX simulation).

burner, and Lagrangian simulations, where the particles are uplifted throughout the domain. To summarize: The particle physics are accurate, the chemistry is not yet so.

3.3 Outlet Conditions

Thus far, a single outlet velocity was presumed sufficient to describe the outlet conditions fully. Figure 5 shows the velocity distribution at the outlet. The solid line represents the velocity distribution calculated in OpenFOAM; a fit to the Poiseuille law is represented by the dot-dashed line. The flow is plug-like, and the boundary layer is under-resolved. The long-dashed and short-dashed lines represent the velocity distributions of the gaseous and solid phases respectively in MFiX. Both show similar trends: near-plug flow along most the of the radius, then a sharp decrease to a non-zero value at the free-slip burner wall. The solids phase is slower than the gaseous phase due to particle inertia. The flow velocity of both phases is lowest at the pipe center: Gravity causes a small number of particles near the centerline to decelerate and even fall back down into the pipe after leaving the outlet. MFiX velocities are lower than OpenFOAM velocities due to higher air temperature, and hence air viscosity, at the outlet in MFiX. Experimental evidence suggests that the particle velocity distribution at the outlet is close to plug flow, particularly near the centre of the pipe [13].

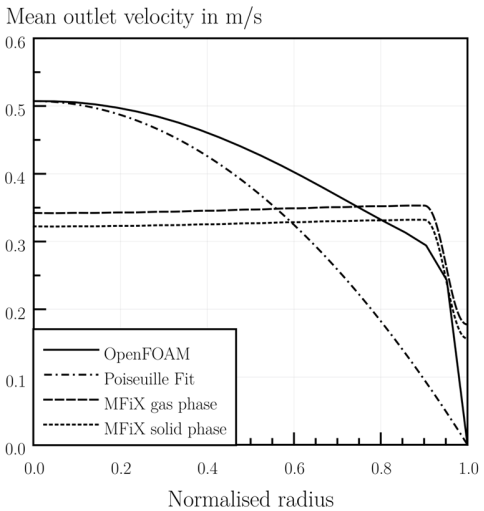


Figure 5: Outlet velocity as a function of the normalized radius in OpenFOAM (solid line), in MFiX of the gas phase (long-dashed line) and in MFiX of the solid phase (short-dashed line). Additionally, the OpenFOAM outlet velocity was fitted to the Poiseuille law (dot-dashed line).

4. Conclusion

An Eulerian model of iron powder combustion was proposed and validated against experimental and Lagrangian work. The model features a sectional representation of the particle size distribution of iron powder, which is also reflected in the kinetics of the oxidation reaction, and was implemented in both single-phase and multiphase CFD. Single-phase CFD broadly matched prior results, though the observed laminar flame speed was shown to differ by an approximate factor of 2, and thus closer to values obtained in microgravity. These discrepancies will not be relevant when scaling up due to high gas velocities and the presence of turbulence. Multiphase simulations displayed accurate granular physics, but the kinetics were lacking. Outlet velocity distributions in both exhibited significant plug-like flow, more so in multiphase simulations.

Going forward, the multiphase implementation will include polydispersity. Then, turbulence will be implemented and validated against experimental work. All these steps are necessary to ensure successful CFD of retrofitted coal-fired power plants.

Declaration of competing interest

The authors declare that they have no known competing financial interests or personal relationships that could have appeared to influence the work reported in this paper.

Acknowledgements

This work was performed in the scope of the DLR project IronCircle® and the cluster project Clean Circles. The authors gratefully acknowledge the scientific support and HPC resources provided by DLR. The HPC system “CARA” used for the CFD simulations in this work is partially funded by the ‘Ministry for Economic Affairs, Labour, Energy, and Climate Protection’ of the Free State of Saxony as well as the ‘Ministry of Research, Technology, and Space’ of the Federal Republic of Germany.

References

[1] J. Janicka, P. Debiagi, A. Scholtissek, A. Dreizler, B. Epple, R. Pawellek, A. Maltsev and C. Hasse, "The potential of retrofitting existing coal power plants: A case study for operation with green iron," Applied Energy, vol. 339, p. 120950, 2023.

[2] J. Neumann, Q. Fradet, A. Scholtissek, F. Dammel, U. Riedel, A. Dreizler, C. Hasse and P. Stephan, "Thermodynamic assessment of an iron-based circular energy economy for carbon-free power supply," Applied Energy, vol. 368, p. 123476, 2024.

[3] T. Hazenberg, D. Braig, M. A. Fedoryk, J. Mich, F. P. Hagen, S. R. Harth, B. Stelzner, A. Scholtissek, D. Trimis and C. Hasse, "Analyzing iron dust bunsen flames using numerical simulations," Fuel, vol. 403, p. 136094, 2026.

[4] F. Gelbard and J. H. Seinfeld, "Simulation of multicomponent aerosol dynamics," Journal of Colloid and Interface Science, vol. 78, no. 2, p. 485–501, 1980.

[5] C. J. Pope and J. B. Howard, "Simultaneous Particle and Molecule Modeling (SPAMM): An Approach for Combining Sectional Aerosol Equations and Elementary Gas-Phase Reactions," Aerosol Science and Technology, vol. 27, no. 1, p. 73–94, 1997.

[6] H. G. Weller, G. Tabor, H. Jasak and C. Fureby, "A tensorial approach to computational continuum mechanics using object-oriented techniques," Computers in Physics, vol. 12, no. 6, p. 620–631, 1998.

[7] Q. Fradet, M. Kurnatowska and U. Riedel, "Thermochemical reduction of iron oxide powders with hydrogen: Review of selected thermal analysis studies," Thermochimica Acta, vol. 726, p. 179552, 2023.

[8] A. Sato, R. Nakagawa, S. Yoshimatsu, A. Fukuzawa and T. Ozaki, "Melting Rate of Iron Oxide Pellets into Iron Melt," Transactions of the Iron and Steel Institute of Japan, vol. 21, no. 12, p. 879–886, 1981.

[9] M. Soo, X. Mi, S. Goroshin, A. J. Higgins and J. M. Bergthorson, "Combustion of particles, agglomerates, and suspensions – A basic thermophysical analysis," Combustion and Flame, vol. 192, p. 384–400, 2018.

[10] J. Mich, D. Braig, T. Gustmann, C. Hasse and A. Scholtissek, "A comparison of mechanistic models for the combustion of iron microparticles and their application to polydisperse iron-air suspensions," Combustion and Flame, vol. 256, p. 112949, 2023.

[11] B.-D. Nguyen, D. Braig, A. Scholtissek, D. Ning, T. Li, A. Dreizler and C. Hasse, "Ignition and kinetic-limited oxidation analysis of single iron microparticles in hot laminar flows," Fuel, vol. 371, p. 131866, 2024.

[12] M. Syamlal, W. Rogers and T. J. O`Brien, MFIX documentation theory guide.

[13] M. Fedoryk, B. Stelzner, S. Harth and D. Trimis, "Experimental investigation of the laminar burning velocity of iron-air flames in a tube burner," Applications in Energy and Combustion Science, vol. 13, p. 100111, 2023.

[14] S. Goroshin, F.-D. Tang, A. J. Higgins and J. H. Lee, "Laminar dust flames in a reduced-gravity environment," Acta Astronautica, vol. 68, no. 7-8, p. 656–666, 2011.